Preliminary Design of the Lean-Combustion Can-type Combustor for the 30-kW Micro gas turbine

Seekharin Komonhirun*, Pisit Yongyingsakthavorn and Udomkiat Nontakeaw

Department of Mechanical and Aerospace Engineering,
King Mongkut's University of Technology North Bangkok, Bangkok, Thailand
*Corresponding author: K.SEEKHARIN@gmail.com

Abstract

This paper presents preliminary results of combustor design for a 30-kW multi-fuel micro gas turbine. To achieve the design conditions, numerical approach is employed to investigate the flow and lean combustion characteristics in the can-type combustor. Its burner part comprises a one-hole fuel injector at the center with an inlet-air swirler placing at prior upstream location. The fuel used is CH_4. Numerical simulation is carried out by using FLUENT. The turbulent and combustion models selected are RNG k-ε and nonpremixed, and compressibility effects are also accounted. Firstly, the effects of combustor size are observed by varying its chamber diameter. The optimum size providing well reverse flow, promoting stabilization of combustion, is then selected to investigate the effects of a swirler angle. It is found that reducing the swirler angle to a certain value leads to more stable fuel-jet reverse flow, better air-fuel mixing, and more stabilized combustion.

***Keywords**: methane, micro gas turbine, lean combustion, swirler angle, FLUENT*

1. Introduction

A micro gas turbine is an interesting candidate for local small power plants. The challenge of micro gas turbine design is to attain its high performance and low environmental impact. A combustor is an important part to achieve not only high performance but also low emissions. In combustor design, swirl flow is a stabilization method broadly applied for both premixed and non-premixed combustion.

There are many researches involving the swirl flow. Man et al. analyzed the flow phenomena inside a low emission stir swirl combustor (LESS) [1]. They indicated that the large recirculation couple of vortex flow is a significant flow pattern for the combustor to increase the combustion enthalpy and reducing NO_x by repeating combustion in vortex flow.

Huang and Yang discovered that the recirculation flow, called a "vortex breakdown", affects to combustion efficiency, and its formation and pattern are dependent on a swirler angle [2]. They also introduced a dimensionless parameter, called "swirl number", relating to the swirl angle. The vortex breakdowns are formed with stable loops when the swirl number is reduced to a certain value. At higher swirl number, the loops tend to be unstable and scatter into a small vortex loops. The swirl number for a radial swirler [3] is given by:

$$S = \frac{\dot{M}^2}{4\pi^2 \rho B R \int_0^R \rho U^2 r dr} \sigma(\phi) \qquad (1)$$

where $\dot{M}$ is a mass flow rate, B is an axial width of an annular channel, R is a radius, U is an axial velocity, $\sigma(\phi)$ is a ratio of mean tangential and radial velocity components at the swirler exit. $\sigma(\phi)$ is a function of a guide vane angles ,ϕ, as:

$$\sigma(\phi) = \frac{1}{1-\psi}\left(\frac{\tan(\phi)}{1+\tan(\phi)\tan\left(\frac{\pi}{z}\right)}\right) \qquad (2)$$

where $\psi = zs/2\pi R_1 \cos\phi$ is a blockage factor from a finite thickness of the guide vanes, z is the number of guide vanes, R_1 is a swirler exit radius and s is the thickness of the guide vanes.

Eldrainy et al. numerically investigated the flow pattern of a radial-swirler can combustor [4]. The results show that the swirl number plays a crucial role on the flow pattern of recirculation at the center of the combustor can. They concluded that the lower swirl number forms a short blunt recirculation loop than the higher. However, increasing swirl number causes larger pressure drop across the swirler. They recommended that the pressure drop should not exceed 10% - 12% for the swirl number around 0.55 - 0.6.

This work aims to numerically investigate reacting flow and lean non-premixed combustion characteristics of the simple designed can-type combustor for different sizes of the combustor and different angles of the swirler.

2. Numerical Analysis

2.1 Governing equation

The governing equations for combustion with turbulent, compressible, dominated-swirl flow are described in this section.

The continuity equation is given by:

$$\frac{\partial \rho}{\partial t} + \nabla(\rho \vec{v}) = 0 \qquad (3)$$

The turbulent model proper to high swirl flow problem is the RNG k-ε equation. The turbulent model RNG k-ε equations are divided into turbulent kinetic energy equation,

$$\frac{\partial}{\partial t}(\rho k) + \frac{\partial}{\partial x_i}(\rho k u_i) = \frac{\partial}{\partial x_j}\left(\alpha_k \mu_{eff} \frac{\partial k}{\partial x_j}\right)$$

$$+G_b + G_k - \rho\epsilon - Y_M \qquad (4)$$

and turbulent dissipation equation,

$$\frac{\partial}{\partial t}(\rho \varepsilon) + \frac{\partial}{\partial x_i}(\rho \varepsilon u_i) = \frac{\partial}{\partial x_j}\left(\alpha_k \mu_{eff} \frac{\partial \varepsilon}{\partial x_j}\right)$$

$$+ C_{1\varepsilon}\frac{\varepsilon}{k}(G_k + C_{3\varepsilon} G_b) - C_{2\varepsilon}\rho\frac{\varepsilon^2}{k} - R_\varepsilon \qquad (5)$$

respectively. For compressible flow, the equation of state of ideal gas is applied:

$$P = \rho R T \qquad (6)$$

For non-premix combustion, the energy equation is derived from total enthalpy of all species as shown by:

$$\frac{\partial}{\partial t}(\rho H) + \nabla \cdot (\rho \vec{v} H) = \nabla \cdot \left(\frac{k_t}{c_p}\nabla H\right) \qquad (7)$$

The two main equations concerning mixture fraction transport and mixture fraction variance transport are demonstrated in Eqs. (8) and (9), respectively.

$$\frac{\partial}{\partial t}(\rho \bar{f}) + \nabla \cdot (\rho \vec{v} \bar{f}) = \nabla \cdot \left(\frac{k_t}{c_p} \nabla \bar{f} \right) \tag{8}$$

$$\frac{\partial}{\partial t}\left(\rho \overline{f'^2}\right) + \nabla \cdot \left(\rho \vec{v} \overline{f'^2}\right) = \nabla \cdot \left(\frac{\mu_t}{\sigma_t} \nabla \overline{f'^2} \right)$$

$$+ C_g \mu_t (\nabla \bar{f})^2 - C_d \rho \frac{\varepsilon}{k} \overline{f'^2} \tag{9}$$

2.2 Model's geometry

Design of the first or baseline model of a non-premixed combustor begins from a simple can-type combustor (see Fig. 1). Its chamber configuration is similar to Khodabandeh's work [5]. However, the burner part and combustion mode are totally different. In this work, combustor design is based on non-premixed burner. The burner part consists of a single-hole fuel nozzle penetrating into a concentric swirling combustion air flow (see Fig. 2).

In this work, the effects of different sizes of the combustor and different angles of the swirler on the reacting flow and non-premixed combustion temperature are numerically investigated. The size of combustor starts with diameter, D = 160 mm, length, L = 200 mm, and swirler angle, θ = 60°. Finally, the lean non-premixed combustion characteristics met the design conditions, such as temperature, pressure, emissions, and enthalpy, are presented.

2.3 Boundary conditions

Boundary conditions applied for numerical simulation include no-slip and adiabatic wall, and non-adiabatic combustion. Fuel type is methane (CH_4) for the preliminary phase of design. The fuel is burnt at lean condition where the equivalent ratio equals 0.6. Table 1 shows other boundary conditions following the design conditions. The ratio of air/fuel Reynolds numbers (Re_{air}/Re_{fuel}) in this work is equal to 0.42 (6,532.35/2,759.28), which is less than 1. This ratio is different from the work done by Janus et al. where the ratio of 1.38 is applied throughout their experiment [6]. Therefore, it is expected that the fuel jet with relative higher level of Re will also plays an important rule on combustion stabilization by its reverse flow.

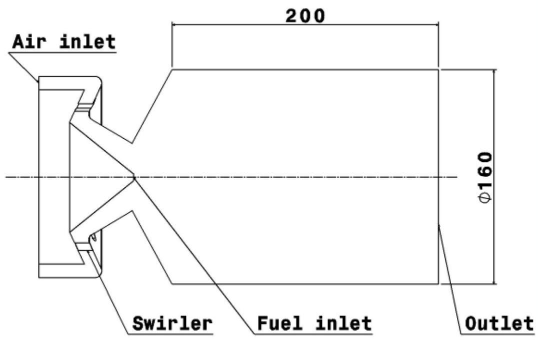

Fig. 1 The baseline can-type combustor

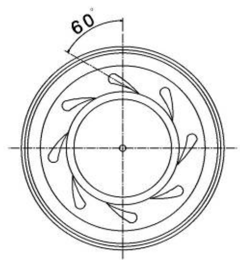

Fig. 2 The swirler of the can-type combustor

2.4 Numerical procedure

The 3-D model of the combustor is generated by using ANYSIS 12.1. The model is then meshed by using the tetrahedral mesh. Numerical solution is conducted by using Fluent 12.1.2.

Table 1 Boundary Conditions

Boundary Condition	Value
1. Air temperature inlet	783 K
2. Exhaust temperature outlet	1089 K
3. Air pressure inlet	4 bar
4. Exhaust pressure outlet	3.5 bar
5. Air mass flow inlet	0.309155 kg/s
6. Fuel mass flow inlet	0.010784 kg/s
7. Fuel temperature inlet	300 K

In this work, the RANS equations with CFD numerical procedures are employed. A steady flow pressure-base solver is applied with added up compressible effects, high swirl flow, and inlet fuel diffusion. All numerical schemes are secondary upwind method. For convergent absolute criteria, iterations and residuals are set equal to 10,000 and 10^{-3}, respectively.

3. Simulation Results and Analysis

3.1 The effects of Combustor Size

Firstly, the combustion simulation for the baseline model with D = 160 cm, L = 200 cm, θ = 60° is performed and the results are shown in Fig. 4. It is clearly seen that the flow are non-axisymmetrical and incredibly disorder (see Fig. 4(a). There are many undesirable vortexes scattering all over the combustion chamber implying that fuel-air mixing is poor and flame is not well stabilized, leading to inefficient combustion performance. Beside of the poor mixing, combustion is not well complete within the chamber because the certain amount of CH_4 does not flow reversely to the burner front leading to insufficient resident time for reaction. This is reflected by the temperature contour in Fig. 4(b). The temperature on the upper part of the chamber is much higher than the lower part and the temperature near the outlet is very high. CH_4 tends to flow upwards, more than downwards, through the small-scale vertexes.

Next, the combustion chamber size is varied to observe its effects. Table 2 shows the different models with different sizes of diameter and length of the combustor. L/D is maintained constant at 1.25 to have geometrical similarity. The results are shown in Figs. 5-7. It is found that the couple of large-scathe le vertexes begin forming at the center when the diameter is increased to 240 mm (Model No. 2). However, the flow is still disorder (see Fig. 5(a)). Temperature contour shows that CH_4 tends to flow downwards more than upwards causing higher temperature on the lower part (see Fig. 5 (b)).

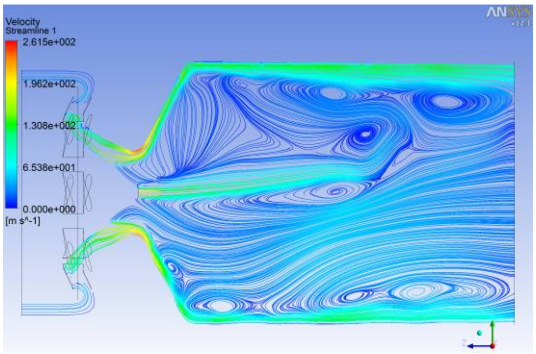

(a) Streamline

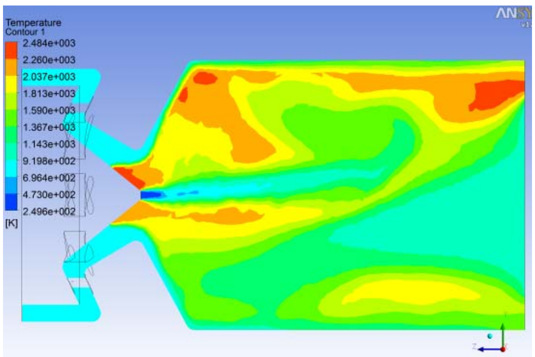

(b) Temperature contour

Fig. 4 The simulation results of the baseline model (D = 160 cm, L = 200 cm, θ = 60°)

Table 2 The different sizes of combustor models

Model No.	Diameter (mm)	Length (mm)	θ (degree)
1	160	200	60°
2	240	300	60°
3	320	400	60°
4	480	600	60°

For Model No. 3, the flow becomes less disorder and is likely to be axisymmetrical pattern with the four large-scale vertexes, two at the center and others near the chamber wall (see Fig. 6(a)). The stable reverse flow of the CH_4 jet provides good distribution of combustion temperature (see Fig. 6 (b)). The high combustion temperature is confined in the area near the burner part. Notice that the fuel jet plays an important rule instead of the swirl air jet at this Re_{air}/Re_{fuel} to induce the recirculation flow.

When the chamber size is further increased, the same flow pattern with Model No. 3 is obtained. The center vertexes are blunter with the larger diameter (Fig. 7 (a)). The temperature distribution is well balanced between the upper and the lower parts of the chamber (Fig. 7 (b)).

Next, the effects of the swirler angle are investigated by using the size of the Model No. 3 combustor as the reference as it is the smallest size providing the stable reverse flow of the CH_4 jet and the good temperature distribution.

3.2 The effects of swirler angle

Table 3 shows the four additional models with different angles of the swirler. The swirler numbers are also calculated and given in the table. Larger the swirl angle, higher the swirl number. The results are shown in the Figs. 8-11.

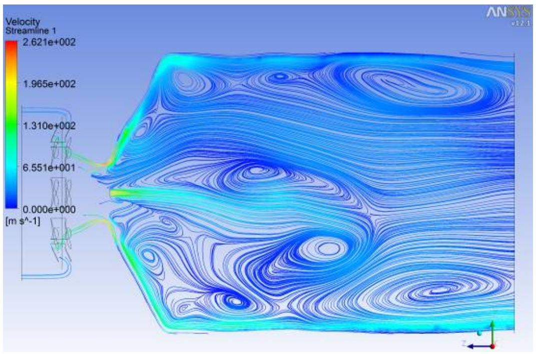

(a) Streamline

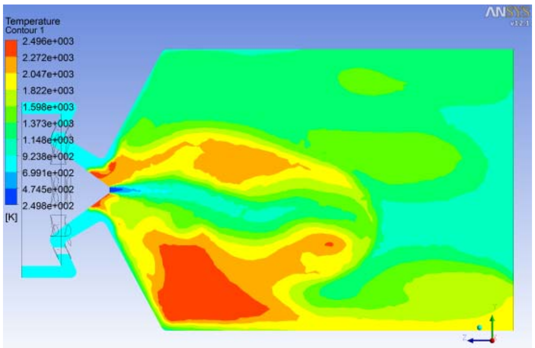

(b) Temperature contour

Fig. 5 The simulation results of Model No. 2 (D = 240 cm, L = 300 cm, θ = 60°)

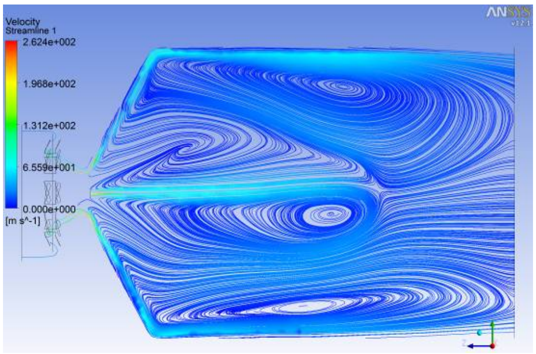

(a) Streamline

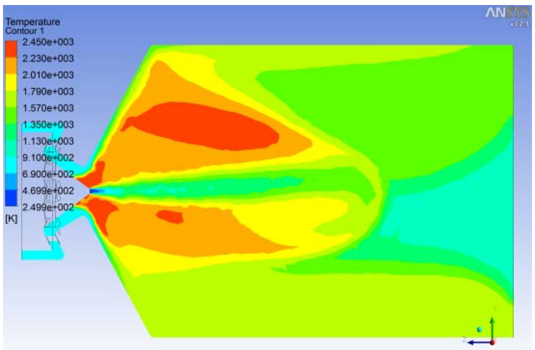

(b) Temperature contour

Fig. 6 The simulation results of Model No. 3 (D = 320 cm, L = 400 cm, θ = 60°)

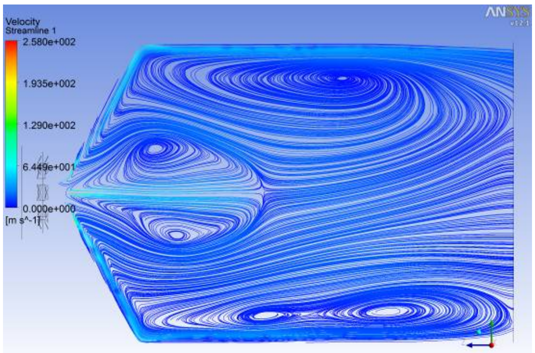

(a) Streamline

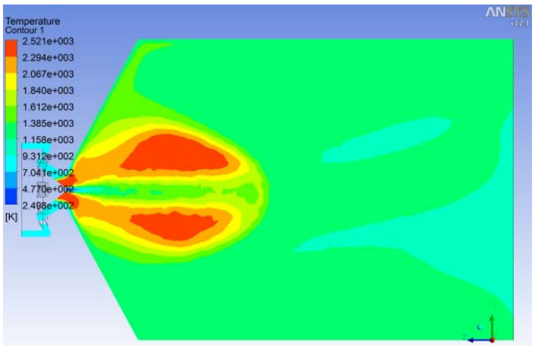

(b) Temperature contour

Fig. 7 The simulation results of Model No. 4 (*D* = 480 cm, *L* = 600 cm, θ = 60°)

Table 3 The different swirler angles

Model No.	Diameter (mm)	Length (mm)	θ (degree)	Swirl number
3	320	400	60°	0.65
5	320	400	65°	0.87
6	320	400	70°	1.35
7	320	400	55°	0.53
8	320	400	50°	0.44

When the swirl number is increased (Model No. 5 and 6), the center vertexes becomes blunter and unstable (see Figs. 8(a) and 9(a)). The higher swirl number provides higher radial velocity and lower axial velocity. The lower axial velocity leads to the deviate jet and disorder flow surrounded by the small-scale vertexes. The temperature distributions become imbalance because of poor stabilization (see Figs. 8(b) and

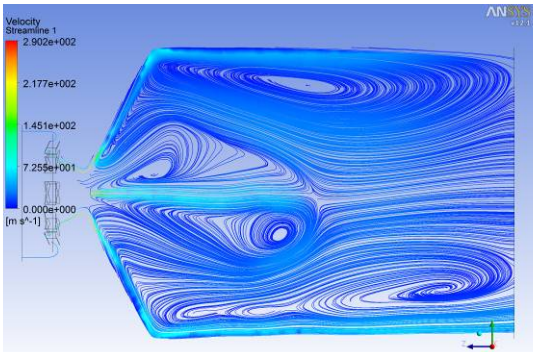

(a) Streamline

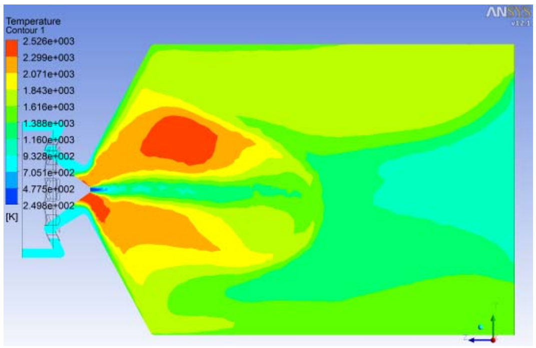

(b) Temperature contour

Fig. 8 The simulation results of Model No. 5 (*D* = 320 cm, *L* = 400 cm, θ = 65°)

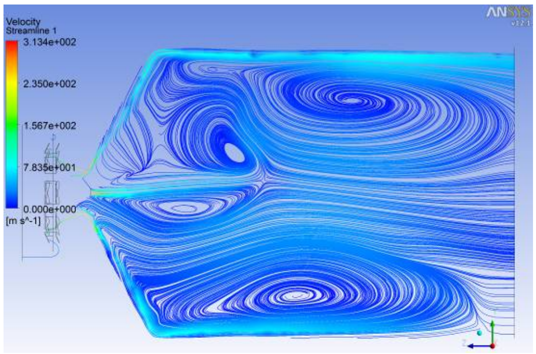

(a) Streamline

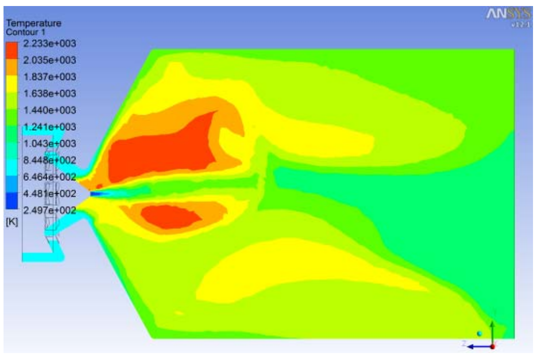

(b) Temperature contour

Fig. 9 The simulation results of Model No. 6 (*D* = 320 cm, *L* = 400 cm, θ = 70°)

9(b)). The results are clearly visible in the case of Model No. 9.

When the swirl number is decreased, the couple of the center vertexes is more acute and stable (see Figs. 10(a) and 11(a)). This is due to the fact that the higher axial velocity promotes the stable reverse flow of the fuel jet. Higher the axial velocity, more stable the reverse flow. The temperature distribution also becomes more balance. This temperature distribution illustrates the good stabilization of combustion (see Figs. 10(b) and 11(b)).

In this work, the optimum combustor providing the good stabilization is the Model No. 8. Table 4 shows the other results at the outlet plane of the combustor. It is found that temperature and pressure are met the design conditions. The amount of CO, OH and CH_4 are sufficiently low. The pressure drop across the swirler is less than 10%, which is the acceptable range [4].

Table 4 The results at the outlet of the combustor

Parameters	Value
Temperature	1361 K
Pressure	3.5 bar
CO_2 molar concentration	5.96×10^{-4} mol/m^3
CO molar concentration	1.55×10^{-6} mol/m^3
O_2 molar concentration	7.23×10^{-3} mol/m^3
OH molar concentration	4.24×10^{-6} mol/m^3
CH_4 molar concentration	4.48×10^{-8} mol/m^3
NO_x mole fraction	1.57×10^{-3} mol/m^3
Enthalpy	707.233 kJ/kg
Total energy	306.909 kJ/kg
Pressure drop	9.5%
Fuel utilization efficiency	61.34%

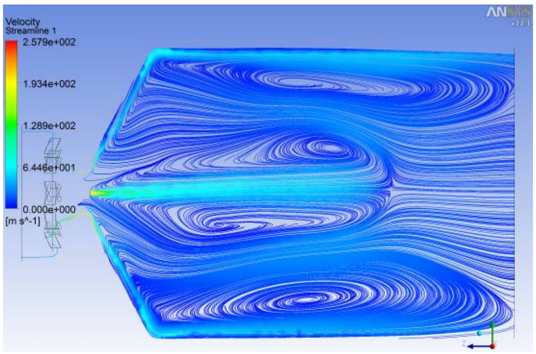

(a) Streamline

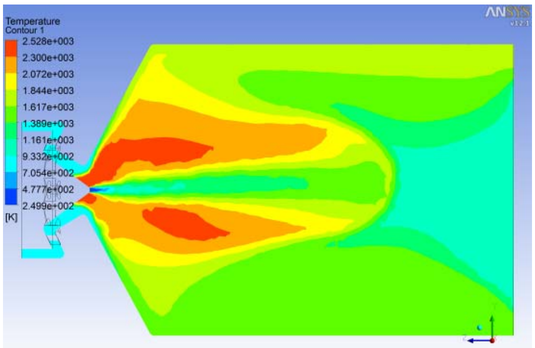

(b) Temperature contour

Fig. 10 The simulation results of Model No. 7 (D = 320 cm, L = 400 cm, θ = 55°)

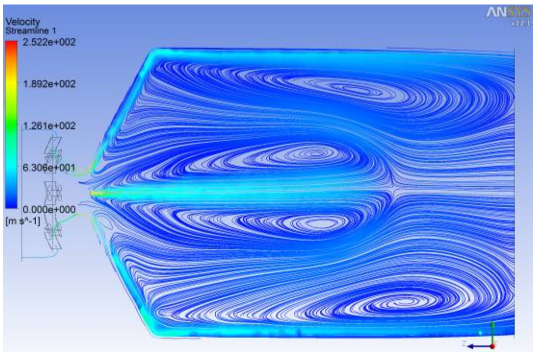

(a) Streamline

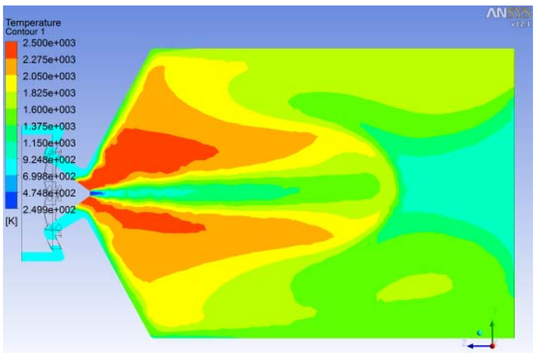

(b) Temperature contour

Fig. 11 The simulation results of Model No. 8 (D = 320 cm, L = 400 cm, θ = 50°)

Lastly, the fuel utilization efficiency is equal to 61.34%. It is calculated by [7]:

$$\eta = \frac{\dot{Q}}{\dot{m}_f LHV} \qquad (10)$$

$$\eta = \frac{-([(A/F)+1]h_{prod}-(A/F)h_a-h_f)}{LHV} \qquad (11)$$

4. Conclusion

From the simulation results of the swirl non-premixed combustion (Re_{air}/Re_{fuel} = 0.42), it can be concluded that:

1. Too small combustor leads to disorder flow where the poor air/fuel mixing and poor stabilization of combustion are obtained. Enlarging the combustor to an appropriate size is required.

2. The swirler angle affects the reverse flow of the fuel jet. The larger angle tends to provide the blunter shape of the couple of the center vertexes. In addition, the too large swirler angle cannot maintain the stable reverse flow of the fuel jet. Reducing the swirler angle to a certain value tends to more stable reverse flow, better air-fuel mixing and more stabilized combustion.

Finally, the optimum combustor met the design conditions here is the combustor with diameter of 320 mm, length of 400 mm and swirler angle of 50°.

5. References

[1] Mana, Z., Zhenbob, F., Yuzhenb, L., and Jibaoa L. (2012). CFD study of NOx emissions in model commercial aircraft engine combustor, *Chinese Journal of Aeronautics*, vol.25, pp. 854 – 863.

[2] Huang, Y. and Yang, V. (2009). Dynamics and stability of lean-premixed swirl stabilized combustion, *Progress in Energy and Combustion Science*, vol.35, pp. 293 -364.

[3] Sheen H.J., Chen W.J., Jen S.Y. and Huang T. L. (1996). Correction of swirl number for radial-type swirl generator, *Experimental Thermal and Fluid Science*, vol.12, pp. 444 – 451.

[4] Eldrainy, Y.A., Ahmad, M.F. and Jaafar, M.N.M. (2009). Investigation of radial swirler effect on flow pattern inside a gas turbine combustor, *Modern Applied Science*, vol.3(5), pp. 21 – 30.

[5] Khodabandeh, A. (2011). CFD modeling of generic gas turbine combustor, Chalmers University of Technology, *Master's Thesis 2011:47*.

[6] Janus, B., Dreizler, A., and Janicka, J. (2007). Experiments on swirl stabilized non-premixed natural gas flames in a model gasturbine combustor, *Proceedings of the Combustion Institute*, vol.31, pp. 3091–3098.

[7] Turns, S.R. (2000). *An introduction to combustion concepts and applications*, 2nd edition, ISBN: 0-07-230096-5, The McGraw-Hill Companies, Inc., Singapore.